

The chemical evolution of self-gravitating primordial disks

Dominik R. G. Schleicher¹, Stefano Bovino², Muhammad A. Latif^{3,4}, Andrea Ferrara^{5,6}, and Tommaso Grassi^{7,8}

¹ Departamento de Astronomía, Facultad Ciencias Físicas y Matemáticas, Universidad de Concepción, Av. Esteban Iturra s/n Barrio Universitario, Casilla 160-C, Concepción, Chile; e-mail: dschleicher@astro-udec.cl

² Institut für Astrophysik, Georg-August-Universität Göttingen, Friedrich-Hund-Platz 1, 37077 Göttingen, Germany

³ Sorbonne Universités, UPMC Univ Paris 06, UMR 7095, Institut d'Astrophysique de Paris, F-75014, Paris, France

⁴ CNRS, UMR 7095, Institut d'Astrophysique de Paris, F-75014, Paris, France

⁵ Scuola Normale Superiore, Piazza dei Cavalieri 7, 56126 Pisa, Italy

⁶ Kavli Institute for the Physics and Mathematics of the Universe (WPI), Todai Institutes for Advanced Study, the University of Tokyo, 5-1-5 Kashiwanoha, Kashiwa, 277-8583, Japan

⁷ Centre for Star and Planet Formation, Natural History Museum of Denmark, Øster Voldgade 5-7, DK-1350 Copenhagen, Denmark

⁸ Niels Bohr Institute, University of Copenhagen, Juliane Maries Vej 30, DK-2100 Copenhagen, Denmark

November 8, 2018

ABSTRACT

Numerical simulations show the formation of self-gravitating primordial disks during the assembly of the first structures in the Universe, in particular during the formation of Pop. III and supermassive stars. Their subsequent evolution is expected to be crucial to determine the mass scale of the first cosmological objects, which depends on the temperature of the gas and the dominant cooling mechanism. Here, we derive a one-zone framework to explore the chemical evolution of such disks and show that viscous heating leads to the collisional dissociation of an initially molecular gas. The effect is relevant on scales of 10 AU (1000 AU) for a central mass of $10 M_{\odot}$ ($10^4 M_{\odot}$) at an accretion rate of $10^{-1} M_{\odot} \text{ yr}^{-1}$, and provides a substantial heat input to stabilize the disk. If the gas is initially atomic, it remains atomic during the further evolution, and the effect of viscous heating is less significant. The additional thermal support is particularly relevant for the formation of very massive objects, such as the progenitors of the first supermassive black holes. The stabilizing impact of viscous heating thus alleviates the need for a strong radiation background as a means of keeping the gas atomic.

1. Introduction

The first stars in the Universe are expected to form from a primordial gas in minihalos of $10^5 - 10^6 M_{\odot}$ at $z = 20 - 30$ (Abel et al. 2002; Bromm & Loeb 2003; Yoshida et al. 2008). Their formation process is often explored from cosmological initial conditions, following the gravitational collapse over many orders of magnitude, to scales of astronomical units (AU) or even below. Due to the characteristic temperatures of ~ 300 K in the primordial gas, the first stars are expected to be considerably more massive than present day stars. Adopting a temperature of ~ 10 K in present-day molecular clouds, one may expect an increase in mass by a factor of $30^{1.5} \sim 140$ based on simple Jeans arguments.

The actual masses and their distribution depend however on the details of the star formation process, which are only partly understood. A central question concerns the role of fragmentation, which may lead to the formation of a stellar cluster rather than a central star (Clark et al. 2008). The latter requires the formation of a self-gravitating disk, and its subsequent fragmentation via gravitational instabilities. Indeed, simulations starting from cosmological initial conditions have now confirmed the formation of self-gravitating disks in minihaloes, as well as their fragmentation (Clark et al. 2011; Greif et al. 2011, 2012; Latif et al. 2013c; Bovino et al. 2014b; Susa et al. 2014). While these

simulations followed the evolution for up to ~ 1000 years depending on resolution, the Kelvin-Helmholtz timescale for a protostar to reach the main sequence is of the order of $\sim 10^6$ years, implying that no final conclusions can be drawn on the properties of the stellar system, and that the simulations so far have only explored the evolution of the disks at very early stages. An exception in this respect are the studies by Hosokawa et al. (2011) and Hirano et al. (2014), who have followed the formation of primordial stars until reaching the main sequence, however at the price of a 2D-approximation. The latter provides a hint towards the final mass distribution, in particular if fragmentation is not efficient or if the resulting clumps efficiently merge with the central object. For a further discussion concerning the state-of-the-art of current simulations exploring Pop. III star formation, we refer to the recent review by Greif (2015).

In massive primordial halos of $10^7 - 10^8 M_{\odot}$, the formation of very massive objects with $\sim 10^5 M_{\odot}$ has been suggested to occur (e.g. Bromm & Loeb 2003; Koushiappas et al. 2004; Lodato & Natarajan 2006; Begelman & Shlosman 2009; Natarajan 2011; Volonteri & Bellovary 2012), as potential progenitors of the observed supermassive black holes at $z \sim 6 - 7$ (Fan et al. 2001; Fan et al. 2004, 2006; Mortlock et al. 2011). In the presence of a strong photo-dissociation background, particularly high temperatures of the gas can be achieved (e.g. Omukai 2001; Schleicher et al.

2010), therefore favoring the formation of very massive primordial objects. Simulations have shown that self-gravitating disks form in haloes cooling via atomic hydrogen (Regan & Haehnelt 2009; Latif et al. 2013a,d; Prieto et al. 2013; Regan et al. 2014; Becerra et al. 2015), where central masses of $10^5 M_{\odot}$ can be reached within 10^4 years after the initial collapse (Latif et al. 2013a).

The black hole mass function resulting from such a direct collapse has been derived by Ferrara et al. (2014) using a semi-analytical approach, considering stellar evolution models for rapidly accreting protostars (Hosokawa et al. 2013; Schleicher et al. 2013). Even for more moderate radiation fluxes, massive stars with $10^3 - 10^4 M_{\odot}$ may still form (Latif et al. 2014b), and the rotational support in disks was found to increase for an increasing amount of molecular cooling (Latif & Volonteri 2015). Also in this context, it is therefore important to understand the long-term evolution of self-gravitating disks both in the atomic and molecular cooling regime.

To complement such numerical investigations, analytical studies have been pursued to investigate the properties of primordial self-gravitating disks. For instance, Lodato & Natarajan (2006) have discussed the role of self-gravitational instabilities and fragmentation during the formation of a massive central black hole, which may be accompanied with a starburst in the self-gravitating disk. Inayoshi & Haiman (2014) have explored the fragmentation properties of a self-gravitating disk cooling via atomic hydrogen, concluding that fragments forming via the gravitational instabilities would subsequently merge with the central object. Latif & Schleicher (2015a) have extended the model into the molecular cooling regime, finding that the merging of clumps is likely still efficient, as the characteristic migration timescales of the clumps are shorter than the timescales of protostellar contraction. In the regime of very massive stars or high accretion rates, the resulting viscous heating may even lead to a transition from the molecular to the atomic cooling regime (Latif & Schleicher 2015b).

Ferrara et al. (2013) have explored the stability of self-gravitating protogalactic disks in the presence of metals, finding that these are subject to strong fragmentation. The latter may provide an obstacle for the formation of massive black holes, as suggested by Mayer et al. (2010, 2014). In the context of self-gravitating protostellar disks, the role of metal and dust cooling has been explored by Tanaka & Omukai (2014), suggesting that they may considerably enhance fragmentation. Similarly, the results of 3D simulations show that fragmentation is triggered by the additional cooling, especially for simulations that are evolved beyond the formation of the first peak. Such behavior has been observed for instance by Clark et al. (2008); Safronek-Shrader et al. (2014); Bovino et al. (2014a); Peters et al. (2014) and Safronek-Shrader et al. (2015).

A substantial debate at this point concerns the question of whether a purely primordial and atomic gas is required for the formation of supermassive black holes, as often assumed in statistical predictions for the high-redshift black hole population (e.g. Dijkstra et al. 2008, 2014; Agarwal et al. 2014). The typical mechanism considered here is the photo-dissociation of molecular hydrogen by Lyman Werner radiation, as explored e.g. by Shang et al. (2010a), which is typically parametrized through a critical radiation flux J_{crit} . Over the last years, it has been shown

that the critical flux can be considerably enhanced by considering realistic stellar spectra (Sugimura et al. 2014; Agarwal et al. 2015), as well as by the dynamics in 3D simulations, where the initial ionization degree is enhanced by shocks and therefore requires an even stronger radiation background to prevent the formation of molecular hydrogen (Latif et al. 2014a, 2015). The simulations suggest a value of J_{crit} of up to 10^5 . For the production of the observed population of $z \sim 6$ black holes, this value is considerably too high, even when considering chemical uncertainties of at most a factor of 5 (Glover 2015).

However, it is by no means clear whether such a critical radiation flux is in fact required for the formation of massive objects. For instance, Begelman & Shlosman (2009) suggested that massive objects could also form from a molecular gas in the presence of self-gravitating instabilities. Simulations by Latif et al. (2014b) confirmed that massive objects of $\sim 10^3 - 10^4 M_{\odot}$ still form for radiation fluxes below J_{crit} , and accretion rates of $\sim 10^{-1} M_{\odot} \text{ yr}^{-1}$ can be maintained even for a moderate radiation background (Latif & Volonteri 2015). In addition, it is conceivable that an atomic gas forms through alternative pathways. For instance, Inayoshi & Omukai (2012) considered the dissociation of the molecular gas by shocks, and showed that the gas would then remain atomic during the further collapse, while Sethi et al. (2010) and Van Borm & Spaans (2013) considered a similar effect due to the dissipation of magnetic energy.

More recently, we found indications that viscous heating in the presence of rotation can substantially heat up the interior of a self-gravitating disk, leading to a transition towards an atomic cooling regime (Latif & Schleicher 2015b). While previous investigations were predominantly exploring a free-fall collapse using one-zone models (e.g. Omukai 2001; Omukai et al. 2005; Glover & Abel 2008; Glover 2015) or the modeling of the early stages of disk formation (e.g. Regan & Haehnelt 2009; Clark et al. 2011; Greif et al. 2011, 2012; Latif et al. 2013c,a; Bovino et al. 2014b; Prieto et al. 2013; Regan et al. 2014; Susa et al. 2014; Becerra et al. 2015), we explore here the chemical and thermal evolution of such disks at their later stages, in particular during the presence of a central massive object. For this purpose, we will consider different disk models and different chemical initial conditions, representing both an initially atomic and an initially molecular gas. For the modeling of the chemistry, we employ the publicly available chemistry package KROME¹ developed by Grassi et al. (2014).

The outline of this paper is as follows. In section 2, we describe the one-zone model for the evolution in a self-gravitating disk in a Lagrangian frame as well as the model for the chemical evolution. In section 3, we present our results for the evolution of disks with an initially molecular gas, and section 4 contains the results for initially atomic disks. A summary and discussion are presented in section 5.

2. Theoretical framework

In the following, we outline a one-zone model to describe the chemical evolution in the mid plane of primordial disks. For this purpose, we assume that the disk is axisymmetric and stationary in an Eulerian reference frame. We then consider

¹ Webpage KROME: <http://kromepackage.org/>

a ring at radius R with mass dM and width dR , implying a surface density $\Sigma = dM/(2\pi R dR)$. In the following, we will consider how the gas in the ring moves inward by adopting a Lagrangian frame of reference and follow its evolution. While the disk is stationary in the Eulerian frame, the gas ring will evolve when moving inward, implying that the density, temperature and chemical abundances will be time-dependent in the Lagrangian frame.

Depending on the mechanism that provides the effective viscosity of the disk, we will in the following describe two models for the evolution of the gas ring. In our first model, we will assume that the viscosity is provided by turbulence and/or magnetic fields, leading to a characteristic surface density profile of $\Sigma \propto 1/R$ in the stationary case, as well as a second model which assumes that the viscosity is provided by gravitational stresses. The latter requires a steeper density profile.

2.1. Generic disk model

As outlined above, we consider a radial annulus of mass dM and surface density Σ at radius R in an axisymmetric primordial disk assumed to be stationary in the Eulerian frame. As a result, the accretion rate \dot{M} is independent of time and position within the disk. The sound speed in the annulus is given as

$$c_s = \sqrt{\gamma k_B T / m}, \quad (1)$$

with k_B the Boltzmann constant, T the gas temperature and m the mean molecular weight. The position and surface density of the annulus under consideration will evolve on the viscous timescale

$$t_{vis} = \frac{R^2}{\nu}, \quad (2)$$

with ν the effective viscosity of the gas. The evolution of radius and surface density is then given by the equations

$$\dot{R} = -\frac{R}{t_{vis}}, \quad (3)$$

$$\dot{\Sigma} = \frac{\Sigma}{t_{vis}}, \quad (4)$$

implying that $\Sigma \propto R^{-1}$. We will refer to this scenario as the "generic disk model". For a stationary disk, the continuity equation reads (Lodato 2007)

$$\dot{M} = 3\pi\nu\Sigma. \quad (5)$$

Under this assumption, the disk viscosity ν follows as

$$\nu = \frac{\dot{M}}{3\pi\Sigma}. \quad (6)$$

While this identity follows from the assumption of stationarity and axisymmetry, such conditions can only be achieved if a physical mechanism is present to provide the effective viscosity ν . In principle, such a viscosity can be provided via turbulence and magnetic fields (see e.g. Balbus & Papaloizou 1999; Hawley 2000). We will initially assume that this is the case, and consider the resulting evolution. The gravitational force in the disk can be dominated either by the central object or by the self-gravity of the disk. As the disk is expected to form via gravitational collapse,

we assume that at least at the initial stage, the Toomre parameter (Toomre 1964)

$$Q \sim \frac{c_s \Omega}{\pi G \Sigma} \quad (7)$$

is of order 1, implying that self-gravity is relevant when the annulus forms. A solution in which $\Sigma \propto R^{-1}$, with $c_s \sim \text{const.}$ and where the self-gravity of the disk dominates over the gravitational force from the central object corresponds to a so-called Mestel disk (Mestel 1963). If the gravitational force is completely balanced by the centrifugal force, the Keplerian angular velocity is given as $\Omega_K = \sqrt{2\pi G \Sigma / R}$ (Lodato 2007). For a realistic disk, we however expect it to be partly supported by thermal and turbulent pressure, as also demonstrated via numerical simulations (e.g. Latif et al. 2013a,c). For the disk-dominated case, we therefore adopt the formulation

$$\Omega_{\text{disk}} = \epsilon_K \sqrt{\frac{2\pi G \Sigma}{R}}, \quad (8)$$

where ϵ_K describes the deviation from a fully rotationally supported disk and G denotes the gravitational constant. We will in the following assume a generic value $\epsilon_K = 50\%$. Assuming $c_s \sim \text{const.}$, $\Sigma \propto R^{-1}$ and Eq. 8, we then have $Q \propto c_s \Omega / \Sigma(R) \propto \sqrt{\Sigma(R)} / R / \Sigma \sim \text{const.} \sim 1$, implying that the disk remains self-gravitating.

For a disk dominated by the central source, we similarly assume that the angular velocity is given as a fraction ϵ_K of the Keplerian rotation, i.e.

$$\Omega_{\text{source}} = \epsilon_K \sqrt{\frac{GM_*}{R^3}}, \quad (9)$$

where M_* denotes the mass of the central source. In this case, it thus follows that $Q \propto c_s \Omega / \Sigma \propto R^{-3/2} / R^{-1} \propto R^{-1/2}$, implying that Q is increasing with decreasing radius, and the interior of the disk becomes gravitationally stable. As long as a sufficient viscosity is provided by turbulence and magnetic fields, the latter is not a problem for the assumed stationarity of the disk. In the next subsection, we will however consider the possibility that the viscosity needs to be provided by self-gravitational instabilities, which will require a steeper relation between Σ and R .

We now calculate the disk height as

$$H = \frac{c_s}{\Omega}. \quad (10)$$

The latter expression holds for gravitationally stable or marginally unstable disks (Lodato 2007), and is thus valid both for $Q \sim 1$ and $Q > 1$. The number density in the mid plane of the disk follows as

$$n = \frac{\Sigma}{2Hm}, \quad (11)$$

and the mass density is given as $\rho = nm$. With these quantities, we can also evaluate the viscous heating rate. The latter is given as (Lodato 2007; Ferrara et al. 2013)

$$Q_+ = \nu \Sigma (R \Omega')^2. \quad (12)$$

The viscous heating rate therefore generally depends on the rotational profile. In case of rotation around a central source, the viscous heating rate can be evaluated as

$$Q_{+, \text{source}} = \frac{9}{4} \nu \Sigma \Omega_{\text{source}}^2. \quad (13)$$

For a disk dominated by self-gravity, on the other hand, we have $\Omega \propto \sqrt{\Sigma/R} \propto R^{-1}$, implying that

$$Q_{+, \text{disk}} = \nu \Sigma \Omega_{\text{disk}}^2. \quad (14)$$

This corresponding heating rate will be employed in the calculation of the chemical and thermal evolution below.

2.2. Self-regulated disk model

As already shown above, a disk dominated by a central source is gravitationally stable in the interior if the evolution of the annulus is dictated by Eqs. 3 and 4, implying $\Sigma \propto R^{-1}$. Such a scenario can thus only be maintained if a sufficient viscosity is provided by turbulence and magnetic fields, as assumed in the generic disk model. However, it is conceivable that gravitational instabilities are required to transport the angular momentum, and they were also shown in previous studies to provide the stronger contribution (e.g. Fromang et al. 2004). While the reality may lie somewhere inbetween, we will explore here the extreme case where self-gravity is necessary to provide the viscosity, requiring that $Q = 1$.

In this model, we assume that the disk is gravitationally unstable on scales larger than the current radius R , implying that gas is transported onto the annulus from larger scales, and the surface density of the annulus keeps increasing as in Eq. 4. The radius R however remains constant as long as $Q > 1$, implying $\dot{R} = 0$, and only evolves as in Eq. 3 if $Q \leq 1$. This condition will effectively alter the relation between Σ and R , and increase the surface density until a state of marginal stability is reached. As a result, one obtains a higher surface density and number density on a given scale, and the ability of the gas to cool increases compared to the generic disk model outlined above.

2.3. Chemical model

To study the chemical evolution for the disk models outlined above, we employ the publicly available chemistry package KROME developed by Grassi et al. (2014). In this framework, we adopt the network "react_primordial3" described by Latif et al. (2015), including the species H, H⁺, H⁻, H₂⁺, H₂, He, He⁺, He⁺⁺ and e⁻. The photo-rates are discarded here, due to the efficiency of self-shielding at high densities. The network includes the currently most accurate rate coefficient for the 3-body H₂ formation derived by Forrey (2013) from on a quantum-mechanical calculation (see also discussion by Bovino et al. 2014c).

The cooling functions in KROME include the atomic line cooling, recombination cooling and Bremsstrahlung cooling as described by Cen (1992), the H₂ cooling function derived by Glover & Abel (2008) as well as the H₂ formation heating and cooling as described by Omukai (2000). Continuum cooling processes are treated as described by Omukai (2000) with the continuum opacities derived by Lenzuni et al. (1991), employing a new fit provided by Grassi et al. (2014). The Lenzuni et al. (1991) opacities include all relevant continuum processes, specifically the bound-free absorption by H and H⁻, free-free absorption by H, H⁻, H₂, H₂⁻, H₂⁺, H₃⁺, He and He⁻, Rayleigh scattering by H, H₂ and He and collisionally-induced absorption by H₂. The viscous heating is included as described in section 2.

The chemical model described here will be called within each dynamical timestep of the disk model outlined above to follow the chemical and thermal evolution. As a result, we obtain the evolution of the chemistry while the gas is moving inward. The latter corresponds to a time sequence in the Lagrangian frame of the annulus, but also describes the structure of the stationary disk in the Eulerian frame. In the following, we will typically show the results as a function of radius to illustrate the resulting structure of the disk.

3. Chemical evolution for an initially molecular gas

In the following, we present the results for the chemical evolution in primordial viscous disks for the scenarios outlined above. For the chemical initial conditions, we consider an initially molecular gas. We adopt a helium fraction of 7.75% with respect to the total number of nuclei. The typical densities at the beginning of the calculation are of the order $\sim 10^9 - 10^{11} \text{ cm}^{-3}$. For a conservative assessment for the impact of viscous heating, we assume here that the gas is very close to fully molecular, with an atomic hydrogen fraction of only 10^{-6} . For the electron/proton abundance, we adopt a generic value of 10^{-9} , which can be expected at such densities (Bovino et al. 2013). The further species abundances like H⁻ and H₂⁺ are initially set to zero, but almost instantaneously reach their equilibrium values during the chemical evolution. We also checked that the results do not strongly depend on these assumptions.

In the following, we will present the chemical evolution for such an initially molecular gas for the case of a generic disk model, both within and without a central source, as well as for a self-regulated disk model, for which we predominantly focus on the case with a central source.

3.1. Results for a generic disk model with no central source

For a generic disk model with no central source, we explore a range of scenarios with different accretion rates, varying between $10^{-3} - 10^0 \text{ M}_{\odot} \text{ yr}^{-1}$, ranging from typical Pop. III star formation (Abel et al. 2002; Bromm & Loeb 2003) to the conditions in atomic cooling haloes (Latif et al. 2013d; Regan et al. 2014). We assume the initial annulus to be at a radius $R = 1000 \text{ AU}$, with a characteristic temperature of $\sim 300 \text{ K}$. The surface densities of the disk are determined via the model of Latif & Schleicher (2015b), implying an initial condition with $Q = 1$. The details of the models are given in Table 1.

| Model | $\dot{M} [\text{M}_{\odot} \text{ yr}^{-1}]$ | $\Sigma [\text{g cm}^{-2}]$ | $R [\text{AU}]$ | $T [\text{K}]$ |
|-------|--|-----------------------------|-----------------|----------------|
| NS0 | 10^0 | 100 | 1000 | 300 |
| NS1 | 10^{-1} | 50 | 1000 | 300 |
| NS2 | 10^{-2} | 25 | 1000 | 300 |
| NS3 | 10^{-3} | 12.5 | 1000 | 300 |

Table 1. Generic disk models with no central source and an initially molecular gas.

As already shown in section 2.1, the surface density scales as R^{-1} under these conditions, and the surface densities reach peak values between 10^5 and 10^6 g cm^{-2} at $R = 1 \text{ AU}$. The results for this case are given in Fig. 1.

We find that the temperature generally increases towards the interior as a result of viscous heating $Q_+ \propto \nu \Sigma \Omega_{\text{disk}}^2$. As $\nu \propto \Sigma^{-1}$ (Eq. 6), the latter essentially scales as $\Omega_{\text{disk}}^2 \propto \Sigma/R \propto R^{-2}$, implying a steep increase as a function of radius, which is only partly compensated by the increasing number density of the gas. In the regime considered here, we note that H_2 is already thermalized, so that the cooling rate only scales linearly with n_{H_2} , and optically depth effects are increasing with density. The gas temperature therefore increases towards values between 1000 – 2000 K, and then rises more gradually.

This behavior is generally found in all cases considered here, with minor deviations for an accretion rate of $0.001 \text{ M}_\odot \text{ yr}^{-1}$, where the gas temperature slightly decreases again near 0.1 AU, as viscous heating is reduced in this case and the collisionally-induced emission (CIE) of molecular hydrogen simultaneously becomes relevant. We further note that the temperature of the gas increases with the accretion rate. This is due to the proportional increase in viscous heating, which is only partly compensated by the increased number densities and the ability of the gas to cool. The viscous heating has therefore a relevant impact on the thermal evolution of the gas, even though the differences in the temperature are here smaller than a factor of 2.

The chemical abundances for a characteristic case with an accretion rate of $0.001 \text{ M}_\odot \text{ yr}^{-1}$ (model NS3) are shown in Fig. 1. We find that the gas is fully molecular during the entire evolution. The atomic hydrogen abundance is initially constant, temporarily increases towards 10^{-2} around $R \sim 1 \text{ AU}$ as a result of the temperature increase, and decreases again in the interior, reflecting the slightly decreasing temperature. Similarly, the proton and electron abundance decreases towards the interior as a result of the increasing densities.

The resulting contributions to heating and cooling are also given in Fig. 1, again for the case of NS3. We note that the viscous heating rate is almost balanced by the molecular hydrogen cooling throughout most of the evolution between 1000 and 1 AU, and subsequently the continuum cooling dominates in the interior. Within $\sim 1 \text{ AU}$, we also find strong chemical heating and cooling, which are however tightly balanced, as the chemistry is close to its equilibrium value. During most of the evolution, the disk remains in the molecular cooling regime, without any strong transitions in the gas temperature.

3.2. Results for a generic disk model with central source

Now, we consider the case of a generic disk model with a central source. For this purpose, we consider stellar masses from $10 - 10^4 \text{ M}_\odot$, ranging from typical Pop. III to supermassive primordial stars, and accretion rates of $10^{-3} - 10^0 \text{ M}_\odot \text{ yr}^{-1}$. We start following the evolution at $R = 1000 \text{ AU}$, taking the initial surface density and gas temperature from the disk model of Latif & Schleicher (2015b). The details of the models are given in Table 2.

In this case, the surface density still scales as R^{-1} , reaching peak values of $10^5 - 10^7 \text{ g cm}^{-2}$. The temperature however changes more significantly during the evolution. For a characteristic case with a stellar mass of 10 M_\odot and an accretion rate of $10^{-3} \text{ M}_\odot \text{ yr}^{-1}$ (model S1A1), the temperature increases from 300 K at $R = 1000 \text{ AU}$ to $\sim 2000 \text{ K}$ at 10 AU, and then raises rapidly to $\sim 7000 \text{ K}$ after only a

| Model | $M_* [\text{M}_\odot]$ | $\dot{M} [\text{M}_\odot \text{ yr}^{-1}]$ | $\Sigma [\text{g cm}^{-2}]$ | $T [\text{K}]$ |
|-------|------------------------|--|-----------------------------|----------------|
| S1A1 | 10^1 | 10^{-1} | 10 | 300 |
| S1A3 | 10^1 | 10^{-3} | 10 | 300 |
| S2A1 | 10^2 | 10^{-1} | 40 | 500 |
| S2A3 | 10^2 | 10^{-3} | 40 | 500 |
| S4A0 | 10^4 | 10^0 | 790 | 1900 |
| S4A1 | 10^4 | 10^{-1} | 630 | 1100 |

Table 2. Models for a generic disk model with central source and an initially molecular gas.

minor change in radius as shown in Fig. 2. This behavior reflects the steep dependence of the viscous heating rate with radius, scaling as $\Omega_{\text{source}}^2 \propto M_*/R^3$. The scaling relation is thus considerably steeper than for the case without a central source, and increases further with increasing stellar mass. Here, the temperature increases towards a value of $\sim 2000 \text{ K}$, where the collisional dissociation of H_2 becomes relevant. We note that the latter has an exponential dependence on the temperature, and therefore the molecular hydrogen becomes fully dissociated after the temperature increases further. At that point, the gas is no longer able to cool via molecular hydrogen, and therefore increases until the heating is balanced via atomic cooling. The temperature then remains high at 6000 – 8000 K on scales below 10 AU.

In general, the evolution is rather similar also for the other cases considered. We note that the transition towards the atomic cooling regime occurs earlier for higher stellar masses and/or higher accretion rates, as both lead to an increase in the amount of viscous heating. For a 10^4 M_\odot star with an accretion rate of $1 \text{ M}_\odot \text{ yr}^{-1}$, the viscous heating is particularly efficient, leading to an almost instantaneous transition already at $R \sim 3000 \text{ AU}$. This transition towards the atomic cooling regime may considerably increase the stability of the accretion disk in the environment of supermassive stars, as also described by Latif & Schleicher (2015b).

The chemical abundances for a representative case with a stellar mass of 100 M_\odot and an accretion rate of $10^{-3} \text{ M}_\odot \text{ yr}^{-1}$ (model S2A3) is given in Fig. 2, clearly showing the transition from the molecular to the atomic regime at $R \sim 30 \text{ AU}$. The latter is accompanied by a significant increase of the ionization fraction due to the higher temperature. We note that the molecular hydrogen abundance starts increasing again with density after the transition, but does not reach values where the H_2 cooling would be significant. In Fig. 2, the heating and cooling rates are plotted for this reference case, confirming that the cooling is initially dominated by molecular hydrogen, and the atomic line cooling takes over after the transition. Within the central 0.3 AU, we note that also chemical heating due to H_2 formation starts getting significant, but is still balanced by the atomic hydrogen cooling. The central temperature then raises to a value of $\sim 9000 \text{ K}$ at 0.1 AU.

3.3. Results for self-regulated disks

As already discussed in section 2.2, it is conceivable that gravitational instabilities are required to provide a sufficiently large effective viscosity to transport the angular momentum, in particular in the regime of high accretion rates.

We therefore consider the evolution in a self-regulated disk, starting with an initially molecular gas. We predominantly focus on the case with a central source. As we mentioned in section 2.1, the evolution in the case without a central source would be very similar to the generic disk model. We explore characteristic masses of the source of $1 - 10^3 M_{\odot}$, including typical Pop. III stars and supermassive stars. Of course, even stronger effects can be expected in case of more massive stars.

We focus here on typical accretion rates of $10^{-1} M_{\odot} \text{ yr}^{-1}$, which is particularly relevant for the formation of supermassive stars in atomic cooling halos. This choice corresponds to a case where viscous heating is particularly relevant. As we have seen in the previous subsection, the characteristic length scale where the transition from molecular to atomic cooling occurs changes by less than a factor of 2 when the accretion rate changes by a factor of 10. We follow the evolution of the disk from a radius of $R = 1000 \text{ AU}$, and evaluate the initial surface density and gas temperature using the model of Latif & Schleicher (2015b). Due to the generally higher surface and number densities in this scenario, we restrict the evolution here to a minimum radius of 1 AU. In fact, considering stellar evolution models for supermassive stars, their typical extend may even exceed such a scale (Hosokawa et al. 2013). Overall, a summary of the scenarios considered here is given in Table 4.

| Model | M_* [M_{\odot}] | \dot{M} [$M_{\odot} \text{ yr}^{-1}$] | Σ [g cm^{-2}] | T [K] |
|-------|-----------------------|---|---------------------------------|---------|
| S1 | 1 | 10^{-1} | 2.5 | 300 |
| S2 | 10 | 10^{-1} | 10 | 400 |
| S3 | 10^2 | 10^{-1} | 40 | 500 |
| S4 | 10^3 | 10^{-1} | 160 | 800 |

Table 4. Models for a self-regulated disk with initially molecular gas.

For the self-gravitating disk models, due to the requirement of $Q = 1$, the resulting relation between surface density Σ and radius R is considerably steeper than for a generic disk model, requiring roughly a relation of $\Sigma \propto R^{-1.5}$. From the results given in Fig. 3, it is evident that characteristic features occur when the temperature increases strongly, i.e. at the transition from the molecular to the atomic cooling regime. In this case, the higher gas temperature needs to be compensated with a higher gas surface density to ensure the condition that $Q = 1$, thus temporarily steepening the relation between surface density and radius.

For a characteristic case with $1 M_{\odot}$ and an accretion rate of $10^{-1} M_{\odot} \text{ yr}^{-1}$ (model S1), the temperature increases first from 400 K at 1000 AU to $\sim 1800 \text{ K}$ at 30 AU, and subsequently increases more gradually, due to the collisional dissociation cooling of molecular hydrogen, towards temperatures above 2000 K near 3 AU, where H_2 becomes fully dissociated and the temperature increases to $\sim 5000 \text{ K}$. A similar behavior is shown for higher stellar masses. This is however more extreme, implying that the transition to the atomic regime occurs earlier, with a higher characteristic temperature. For instance in the case of a supermassive star with $10^3 M_{\odot}$, the transition to the atomic regime occurs already at 300 AU, with a peak temperature of 7000 K.

For our reference model S1, the evolution of the species abundances is given in Fig. 3, confirming the transition from the molecular to the atomic regime near 10 AU as well as the subsequent build-up of molecular hydrogen due to the high densities of the gas. It therefore starts affecting the cooling again around densities of 10^{16} cm^{-3} . The viscous heating is initially balanced by the molecular cooling between 30 and 1000 AU. Between 30 and 3 AU, the main cooling channel is due to H_2 collisional dissociation cooling. In the central 3 AU, the contributions of viscous heating, continuum cooling as well as chemical heating and cooling strongly balance each other, and molecular hydrogen line cooling starts playing some role due to the increasing H_2 abundance. However, it is also visible for instance in the case S2 that the H_2 abundance is collisionally dissociated, as the critical temperature for H_2 dissociation decreases with density and the disk evolves into a denser regime. We expect similar effects to occur in the scenarios S3 and S4, where the calculation becomes however numerically unstable at this point as a result of the stronger viscous heating.

4. Chemical evolution for an initially atomic gas

Now, we consider a case where the gas in the disk is initially atomic. In this case, we adopt an initial molecular hydrogen abundance of 10^{-6} and an initial temperature of 10^4 K . Due to the higher temperature, we also assume an increased ionization degree of 10^{-6} . In the following, we present the chemical evolution for an initially atomic gas both in the case of a generic disk model, as well as for a self-regulated disk.

4.1. Results for a generic disk model with and without central source

For the case of a generic disk model, we consider scenarios with and without a central source, with source masses of $10 - 10^4 M_{\odot}$. We adopt here an accretion rate of $10^{-1} M_{\odot} \text{ yr}^{-1}$ to explore a case where viscous heating is particularly relevant. We start with a characteristic surface density of 10 g cm^{-2} at 1000 AU. We note that these disks are not necessarily self-gravitating, in particular in the presence of a central source, and the viscosity to build up the disk thus needs to be provided by turbulence or (magneto-)hydrodynamical instabilities. A summary of the explored models is given in Table 5.

| Model | M_* [M_{\odot}] | \dot{M} [$M_{\odot} \text{ yr}^{-1}$] | Σ [g cm^{-2}] | T [K] |
|-------|-----------------------|---|---------------------------------|---------|
| H0 | 0 | 10^{-1} | 10 | 10^4 |
| H1 | 10 | 10^{-1} | 10 | 10^4 |
| H2 | 100 | 10^{-1} | 10 | 10^4 |
| H3 | 10^4 | 10^{-1} | 10 | 10^4 |

Table 5. Models for a generic disk model with an initially atomic gas.

The evolution of the gas temperature as a function of radius is given in Fig. 4. The temperature remains high throughout the entire evolution, from $R = 1000 \text{ AU}$ to $R = 0.1 \text{ AU}$, but decreases slightly from initially 8000 – 9000 K to 6000 – 9000 K in the interior. We note that the temperature slightly increases with central mass as a result of

| Abbreviation | cooling and heating terms | reference |
|----------------|--|-----------------------|
| viscous | viscous heating | Lodato (2007) |
| chem. | net chemical heating / cooling due | Omukai (2000) |
| chem. heat | chemical heating due to H ₂ formation | Omukai (2000) |
| chem. cool | chemical cooling due to H ₂ dissociation | Omukai (2000) |
| atomic | atomic line cooling, recombination cooling, Bremsstrahlung | Cen (1992) |
| H ₂ | H ₂ line cooling | Glover & Abel (2008) |
| cont | continuum cooling | Lenzuni et al. (1991) |

Table 3. Cooling and heating functions listed under different abbreviations in Figs. 1, 2, 3, 4 and 5.

the enhanced viscous heating. The role of viscous heating is overall less pronounced compared to the initially molecular regime, as also found by Ferrara et al. (2013). In fact, the temperature remains high even in the absence of a central source, though may somewhat increase in the presence of viscous heating.

For a characteristic case with a central source of $10 M_{\odot}$ and an accretion rate of $10^{-1} M_{\odot} \text{ yr}^{-1}$ (model H1), the resulting species abundances are plotted in Fig. 4. We note that the gas is atomic in the entire regime, and H₂ remains strongly suppressed via collisional dissociation due to the high temperature. Within the central 10 AU, the H₂ abundance starts increasing due to a mild decrease of the temperature, however leading only to an abundance of 10^{-4} at 0.1 AU, which is insufficient to drive the cooling. The ionization degree only evolves very gradually as a function of radius, and is slightly decreasing due to the increasing densities. The viscous heating is balanced by the atomic cooling through almost the entire evolution. Only in the very central 0.3 AU, chemical heating via three-body H₂ formation becomes important as well, but is still balanced by the atomic line cooling. The molecular hydrogen cooling remains negligible throughout the entire evolution.

4.2. Results for self-regulated disks

Now, we finally explore the chemical evolution of initially atomic disks in a self-regulated scenario with $Q = 1$. In this regime, we focus again on the case with a central source, as otherwise the evolution would be very similar to the case of a generic disk model. We consider here central sources with masses of $1 - 10^3 M_{\odot}$, and characteristic accretion rates of $10^{-1} M_{\odot} \text{ yr}^{-1}$. We start with an initial surface density of 10 g cm^{-2} , which however adjusts early in the evolution due to the requirement of $Q = 1$. Due to the generally higher surface and number densities in this scenario, we restrict the evolution here to a minimum radius of 1 AU. In fact, considering stellar evolution models for supermassive stars, their typical extend may even exceed such a scale (Hosokawa et al. 2013). The overall models considered here are summarized in Table 6.

| Model | M_* [M_{\odot}] | \dot{M} [$M_{\odot} \text{ yr}^{-1}$] | Σ [g cm^{-2}] |
|-------|-----------------------|---|---------------------------------|
| HS0 | 1 | 10^{-1} | 10 |
| HS1 | 10 | 10^{-1} | 10 |
| HS2 | 100 | 10^{-1} | 10 |
| HS3 | 10^3 | 10^{-1} | 10 |

Table 6. Models for a self-regulated disk with initially atomic gas.

The surface density of the gas as a function of radius is given in Fig. 5, showing that the surface density profile clearly steepens compared to a generic disk model, requiring a scaling as $\Sigma \propto R^{-1.5}$. Different from the case with initially molecular cooling, the profile strongly resembles a power-law with no particular features, as the temperature evolution is generally more gradual and mostly without strong transitions. The temperature initially remains high, while some continuum cooling may set in between 60 and 10 AU. The temperature then decreases more steeply towards $\sim 3000 \text{ K}$. For central sources with 1 and $10 M_{\odot}$, we find that the temperature subsequently increases again, as a result of viscous heating and H₂ collisional dissociation. For higher central masses, the calculation becomes unstable at the point of this transition, due to the correspondingly higher heating and cooling rates. In principle, we expect however a similar evolution.

The chemical evolution is given for a characteristic case with a central source of $1 M_{\odot}$ and an accretion rate of $10^{-1} M_{\odot} \text{ yr}^{-1}$, corresponding to model HS0. While the gas is atomic in the entire range, the H₂ abundance increases significantly from $\sim 10^{-9}$ at $\sim 50 \text{ AU}$, reaching a peak value close to 0.1 at 1 AU. The ionization degree initially decreases only slightly with density between 1000 and 10 AU, and then drops more significantly towards 10^{-12} due to the lower temperatures.

As shown in Fig. 5, the viscous heating is balanced by atomic hydrogen cooling between 1000 and 30 AU. In the interior, the contribution of the continuum cooling is subsequently close to the viscous heating. In this regime, the chemical heating and cooling as well as the contributions of viscous heating and continuum cooling strongly balance each other, and the temperature decrease is driven by the molecular hydrogen cooling. The characteristic temperature for H₂ dissociation however depends on the density, and the critical point for H₂ dissociation is indeed reached at $R \sim 1 \text{ AU}$, leading to the dissociation of molecular hydrogen and a resulting increase of the temperature.

Also in this case, the role of viscous heating is therefore less pronounced for the initially atomic than for the initially molecular regime. However, due to the higher gas densities in the self-gravitating regime, the H₂ formation is enhanced for these cases, so that the cooling is initially somewhat enhanced, and the viscous heating prevents the gas from becoming molecular again in the central 1 – 10 AU, therefore somewhat contributing to the stability in the very central region. This behavior concerns relatively small scales. A supermassive star with $\sim 10^4 M_{\odot}$ may already have radii up to $\sim 100 \text{ AU}$ (Hosokawa et al. 2013), providing a natural cut-off for the inner disk. It thus appears likely that the viscous heating has only a minor effect in the initially atomic regime.

5. Summary and discussion

We have developed a one-zone framework to describe the chemical and thermal evolution of primordial disks depending on the mechanism which provides the viscosity of the disk. Assuming a sufficient viscosity is always available as a result of turbulence and/or magnetic fields (see e.g. Balbus & Papaloizou 1999; Hawley 2000), we have derived the generic disk model under the assumption of stationarity and axisymmetry, leading to a characteristic power-law profile of the surface density Σ scaling as $1/R$. Under these assumptions, the effective viscosity of the disk follows from the requirement to maintain the accretion rate and the transport of angular momentum, therefore providing the amount of viscous heating (see e.g. Lodato 2007; Inayoshi & Haiman 2014; Latif & Schleicher 2015a). We further distinguish between scenarios where the rotation profile is determined by the self-gravity of the disk, as well as scenarios where gravity is dominated by the central source.

If rotation is dominated by the central source, it follows that the disk becomes gravitationally stable on smaller scales due to the relation $\Sigma \propto R^{-1}$. In particular in the regime of high accretion rates, one may however expect that self-gravity contributes significantly to the transport of angular momentum (e.g. Begelman & Shlosman 2009). We therefore consider also a self-regulated disk model, in which the disk viscosity is due to gravitational instabilities, therefore requiring a scenario with the Toomre $Q \sim 1$. In these cases, we obtain a steeper profile for the surface density of the disk in a marginally stable state. We refer here to Lodato (2007) for a review on the properties of such disks.

The resulting evolution has been explored for a range of stellar masses and accretion rates, considering both conventional Pop. III star formation (e.g. Abel et al. 2002; Bromm & Loeb 2003; Yoshida et al. 2008) as well as the formation of supermassive primordial stars (e.g. Lodato & Natarajan 2006; Regan & Haehnelt 2009; Latif et al. 2013b; Ferrara et al. 2014). As chemical initial conditions, we have both explored an initially molecular gas, as expected for instance in minihalos (e.g. Abel et al. 2002; Bromm & Loeb 2003; Yoshida et al. 2008), as well as an initially atomic gas. In more massive haloes, the chemical evolution depends on the ambient radiation background, and is typically molecular for moderate values and atomic for very strong values of the radiation background (e.g. Omukai 2001; Greif et al. 2008; Shang et al. 2010b; Schleicher et al. 2010; Latif et al. 2011, 2015).

In case of the initially molecular gas, we find that viscous heating plays a crucial role in the presence of a central source and accretion rates of $\sim 10^{-1} M_{\odot} \text{ yr}^{-1}$, both for the generic and the self-regulated disk model. For a central star with about $10 M_{\odot}$, the viscous heating leads to the collisional dissociation of molecular hydrogen on scales of ~ 10 AU, and the effect is further enhanced for supermassive stars with $\sim 10^4 M_{\odot}$, where the molecular gas is dissociated already on scales of ~ 1000 AU. The latter thus strongly contributes to the stabilization of the central region. Even if fragmentation occurs, the resulting clumps will be more massive, and are expected to rapidly migrate towards the central region (Inayoshi & Haiman 2014; Latif & Schleicher 2015b). However, fragmentation may be more efficient on larger scales where the gas is molecular, and also the migration time is increasing with the

distance from the central object. It is thus certainly viable that fragmentation occurs on some scale, which could potentially contribute to the formation of a starburst ring around the central object (Lodato & Natarajan 2006). In such a case, the further accretion may be regulated by the interplay of gravitational instabilities with stellar feedback (Kawakatu & Wada 2009; Wutschik et al. 2013).

We further explored the case where the gas is initially atomic. In case of the generic disk model, it then remains atomic, as collisional dissociation of molecular hydrogen is efficient at the temperatures of atomic hydrogen cooling (Inayoshi & Omukai 2012). Due to the high temperatures, the overall cooling rates are considerably enhanced, and the effect of viscous heating is therefore less relevant in this regime, as also described by Ferrara et al. (2013) for a hot metal-enriched gas. In the case of a self-gravitating disk model, we find that some H_2 may build up again towards the central region, due to the higher densities obtained in this regime. However, the characteristic temperatures are still above ~ 3000 K throughout the evolution. As the characteristic temperature for H_2 collision dissociation decreases with increasing density, we find that the H_2 dissociates again after an initial build-up. Overall, the gas essentially remains atomic for most of the evolution.

The potential impact of viscous heating is well-known for instance in the case of quasar accretion disks, where the resulting heat input leads to the presence of a hot gas over a large range of scales (e.g. Goodman 2003; Goodman & Tan 2004). In the context of primordial star formation, such effects have not been strongly considered. The one-zone models exploring the chemical evolution have typically assumed a free-fall collapse (e.g. Omukai 2001; Omukai et al. 2005; Glover & Abel 2008; Glover 2015), while simulations were usually restricted to the early stages of disk formation. For instance, Clark et al. (2011) were following the evolution until $\sim 1 M_{\odot}$ of mass had turned into stars, while Greif et al. (2011) stopped the evolution when a $\sim 10 M_{\odot}$ star was formed, still with a moderate accretion rate of $10^{-2} M_{\odot}$. In a follow-up investigation at higher resolution, they evolved the simulation until stellar masses of $\sim 1 M_{\odot}$, and noted that heating both due to the accretion onto the protostar, as well as due to shocks close to the spiral arm has occurred (Greif et al. 2012). It is conceivable that these are the first signatures of viscous heating, even though still at an early stage. In the context of supermassive stars, we note that the majority of runs already started from an atomic gas, which typically remained atomic during the further evolution (e.g. Regan & Haehnelt 2009; Latif et al. 2013a,d; Prieto et al. 2013; Regan et al. 2014; Becerra et al. 2015). The longer-term evolution in the presence of molecular cooling has been explored in simulations by Latif et al. (2014b) and Latif & Volonteri (2015), showing that high accretion rates can be maintained, but without resolving the scales considered here.

The results obtained here are particularly important for the formation of massive central object, as the enhanced temperature in the atomic gas increases the stability in the interior of the disk and helps to maintain a high accretion rate. The latter also alleviates the need of a strong external radiation field, typically expressed through a critical value J_{crit} , as a means of providing an atomic gas. We expect these results to be particularly relevant in the case of massive central objects of at least $10 M_{\odot}$ and high accretion rates of $\sim 10^{-1} M_{\odot} \text{ yr}^{-1}$. The nature of the phenomenon

discussed here, and in particular the characteristic scaling of the viscous heating rate as R^{-3} leads us to the expectation that such a transition should generally occur, even though it may be shifted for instance if the surface density is enhanced and thus also the ability of the gas to cool. Even in the case of fragmentation and a more turbulent flow, we expect that gas velocities of the order of the Keplerian velocity will occur, leading to the formation of strong shocks and a transition towards the atomic cooling regime.

Of course, the models here are still based on simplifying assumptions, such as the stationarity and axisymmetry of the disk, which can only hold at an approximate level. It is therefore important to investigate the evolution in such disks in 3D simulations following the interplay of chemistry, heating and cooling along with the gravitational dynamics to assess the impact on fragmentation. For such time-dependent models, the viscosity of the disk can no longer be obtained from the assumption of stationarity, but one may have to adopt explicit parametrizations of the viscosity in self-gravitating disks as derived for instance by Rafikov (2015). Due to the timescales involved in the evolution of such disks, we expect that the latter can not be pursued in cosmological simulations, but that independent studies are needed to investigate the stability of self-gravitating primordial disks with already a massive protostar. Depending on the mass and accretion rate of the protostar, also radiation feedback may become relevant, even though it may predominantly affect the regions outside the disk (e.g. Hosokawa et al. 2011; Hirano et al. 2014). In the case of rapid accretion, it was found that the UV feedback from protostars is likely negligible, as they are expected to have cool atmospheres like a red giant (Hosokawa et al. 2013; Schleicher et al. 2013).

Beyond the primordial case, the influence of dust cooling is potentially significant at high densities (e.g. Schneider et al. 2003; Omukai et al. 2005; Schneider et al. 2006; Omukai et al. 2008; Cazaux & Spaans 2009; Dopcke et al. 2011, 2013; Schneider et al. 2012). However, most of these investigations have employed one-zone models assuming a free-fall collapse, while we have shown here that the heating mechanism is considerably different in a rotating disk around a central protostar. In this regime, the role of dust cooling requires further investigations, to understand the fragmentation behavior at the later stages of the evolution. The latter can be important both for the formation of the first low-mass stars (e.g. Schneider et al. 2012; Klessen et al. 2012), but also for the formation scenarios of massive black holes (Omukai et al. 2008; Ferrara et al. 2013). Even if fragmentation occurs, a black hole may possibly form, as long as the cluster is fed via substantial inflows and gravitational instabilities occur (Alexander & Natarajan 2014).

Acknowledgements. DRGS and SB thank for funding through the DFG priority program "The Physics of the Interstellar Medium" (projects SCHL 1964/1-1, SCHL 1964/1-2 and BO 4113/1-2). ML received funding from the "BLACK" project funded via the European Research Council under the European Community's Seventh Framework Programme (FP7/2007-2013 Grant Agreement no. 614199, project "BLACK"). TG acknowledges the Centre for Star and Planet Formation funded by the Danish National Research Foundation.

References

Abel, T., Bryan, G. L., & Norman, M. L. 2002, *Science*, 295, 93

- Agarwal, B., Dalla Vecchia, C., Johnson, J. L., Khochfar, S., & Paardekooper, J.-P. 2014, *MNRAS*, 443, 648
- Agarwal, B., Smith, B., Glover, S., Natarajan, P., & Khochfar, S. 2015, ArXiv e-prints
- Alexander, T. & Natarajan, P. 2014, *Science*, 345, 1330
- Balbus, S. A. & Papaloizou, J. C. B. 1999, *ApJ*, 521, 650
- Becerra, F., Greif, T. H., Springel, V., & Hernquist, L. E. 2015, *MNRAS*, 446, 2380
- Begelman, M. C. & Shlosman, I. 2009, *ApJ*, 702, L5
- Bovino, S., Grassi, T., Latif, M. A., & Schleicher, D. R. G. 2013, *MNRAS*, 434, L36
- Bovino, S., Grassi, T., Schleicher, D. R. G., & Latif, M. A. 2014a, *ApJ*, 790, L35
- Bovino, S., Latif, M. A., Grassi, T., & Schleicher, D. R. G. 2014b, *MNRAS*, 441, 2181
- Bovino, S., Schleicher, D. R. G., & Grassi, T. 2014c, *A&A*, 561, A13
- Bromm, V. & Loeb, A. 2003, *ApJ*, 596, 34
- Cazaux, S. & Spaans, M. 2009, *A&A*, 496, 365
- Cen, R. 1992, *ApJS*, 78, 341
- Clark, P. C., Glover, S. C. O., & Klessen, R. S. 2008, *ApJ*, 672, 757
- Clark, P. C., Glover, S. C. O., Smith, R. J., et al. 2011, *Science*, 331, 1040
- Dijkstra, M., Ferrara, A., & Mesinger, A. 2014, *MNRAS*, 442, 2036
- Dijkstra, M., Haiman, Z., Mesinger, A., & Wyithe, J. S. B. 2008, *MNRAS*, 391, 1961
- Dopcke, G., Glover, S. C. O., Clark, P. C., & Klessen, R. S. 2011, *ApJ*, 729, L3
- Dopcke, G., Glover, S. C. O., Clark, P. C., & Klessen, R. S. 2013, *ApJ*, 766, 103
- Fan, X., Hennawi, J. F., Richards, G. T., et al. 2004, *AJ*, 128, 515
- Fan, X., Strauss, M. A., Richards, G. T., et al. 2006, *AJ*, 131, 1203
- Fan et al. 2001, *AJ*, 122, 2833
- Ferrara, A., Haardt, F., & Salvaterra, R. 2013, *MNRAS*, 434, 2600
- Ferrara, A., Salvadori, S., Yue, B., & Schleicher, D. 2014, *MNRAS*, 443, 2410
- Forrey, R. C. 2013, *ApJ*, 773, L25
- Fromang, S., Balbus, S. A., Terquem, C., & De Villiers, J.-P. 2004, *ApJ*, 616, 364
- Glover, S. C. O. 2015, ArXiv e-prints 1504.00514
- Glover, S. C. O. & Abel, T. 2008, *MNRAS*, 388, 1627
- Goodman, J. 2003, *MNRAS*, 339, 937
- Goodman, J. & Tan, J. C. 2004, *ApJ*, 608, 108
- Grassi, T., Bovino, S., Schleicher, D. R. G., et al. 2014, *MNRAS*, 439, 2386
- Greif, T. H. 2015, *Computational Astrophysics and Cosmology*, 2, 3
- Greif, T. H., Bromm, V., Clark, P. C., et al. 2012, *MNRAS*, 424, 399
- Greif, T. H., Johnson, J. L., Klessen, R. S., & Bromm, V. 2008, *MNRAS*, 387, 1021
- Greif, T. H., Springel, V., White, S. D. M., et al. 2011, *ApJ*, 737, 75
- Hawley, J. F. 2000, *ApJ*, 528, 462
- Hirano, S., Hosokawa, T., Yoshida, N., et al. 2014, *ApJ*, 781, 60
- Hosokawa, T., Omukai, K., Yoshida, N., & Yorke, H. W. 2011, *Science*, 334, 1250
- Hosokawa, T., Yorke, H. W., Inayoshi, K., Omukai, K., & Yoshida, N. 2013, *ApJ*, 778, 178
- Inayoshi, K. & Haiman, Z. 2014, *MNRAS*, 445, 1549
- Inayoshi, K. & Omukai, K. 2012, *MNRAS*, 422, 2539
- Kawakatu, N. & Wada, K. 2009, *ApJ*, 706, 676
- Klessen, R. S., Glover, S. C. O., & Clark, P. C. 2012, *MNRAS*, 421, 3217
- Kouchiappas, S. M., Bullock, J. S., & Dekel, A. 2004, *MNRAS*, 354, 292
- Latif, M. A., Bovino, S., Grassi, T., Schleicher, D. R. G., & Spaans, M. 2015, *MNRAS*, 446, 3163
- Latif, M. A., Bovino, S., Van Borm, C., et al. 2014a, *MNRAS*, 443, 1979
- Latif, M. A. & Schleicher, D. R. G. 2015a, *MNRAS*, 449, 77
- Latif, M. A. & Schleicher, D. R. G. 2015b, *A&A*, accepted (ArXiv e-prints 1411.5902)
- Latif, M. A., Schleicher, D. R. G., Bovino, S., Grassi, T., & Spaans, M. 2014b, *ApJ*, 792, 78
- Latif, M. A., Schleicher, D. R. G., Schmidt, W., & Niemeyer, J. 2013a, *MNRAS*, 433, 1607
- Latif, M. A., Schleicher, D. R. G., Schmidt, W., & Niemeyer, J. 2013b, *MNRAS*, 433, 1607
- Latif, M. A., Schleicher, D. R. G., Schmidt, W., & Niemeyer, J. 2013c, *ApJ*, 772, L3
- Latif, M. A., Schleicher, D. R. G., Schmidt, W., & Niemeyer, J. C. 2013d, *MNRAS*, 436, 2989

Latif, M. A., Schleicher, D. R. G., Spaans, M., & Zaroubi, S. 2011, *A&A*, 532, A66

Latif, M. A. & Volonteri, M. 2015, ArXiv e-prints 1504.00263

Lenzuni, P., Chernoff, D. F., & Salpeter, E. E. 1991, *ApJS*, 76, 759

Lodato, G. 2007, *Nuovo Cimento Rivista Serie*, 30, 293

Lodato, G. & Natarajan, P. 2006, *MNRAS*, 371, 1813

Mayer, L., Fiacconi, D., Bonoli, S., et al. 2014, ArXiv e-prints 1411.5683

Mayer, L., Kazantzidis, S., Escala, A., & Callegari, S. 2010, *Nature*, 466, 1082

Mestel, L. 1963, *MNRAS*, 126, 553

Mortlock et al. 2011, *Nature*, 474, 616

Natarajan, P. 2011, The formation and evolution of massive black hole seeds in the early Universe, ed. D. J. Saikia & V. Trimble (World Scientific Publishing Co), 191–206

Omukai, K. 2000, *ApJ*, 534, 809

Omukai, K. 2001, *ApJ*, 546, 635

Omukai, K., Schneider, R., & Haiman, Z. 2008, *ApJ*, 686, 801

Omukai, K., Tsuribe, T., Schneider, R., & Ferrara, A. 2005, *ApJ*, 626, 627

Peters, T., Schleicher, D. R. G., Smith, R. J., Schmidt, W., & Klessen, R. S. 2014, *MNRAS*, 442, 3112

Prieto, J., Jimenez, R., & Haiman, Z. 2013, *MNRAS*, 436, 2301

Rafikov, R. R. 2015, ArXiv e-prints 1501.04980

Regan, J. A. & Haehnelt, M. G. 2009, *MNRAS*, 396, 343

Regan, J. A., Johansson, P. H., & Haehnelt, M. G. 2014, *MNRAS*, 439, 1160

Safranek-Shrader, C., Milosavljević, M., & Bromm, V. 2014, *MNRAS*, 438, 1669

Safranek-Shrader, C., Montgomery, M., Milosavljevic, M., & Bromm, V. 2015, ArXiv e-prints 1501.03212

Schleicher, D. R. G., Palla, F., Ferrara, A., Galli, D., & Latif, M. 2013, *A&A*, 558, A59

Schleicher, D. R. G., Spaans, M., & Glover, S. C. O. 2010, *ApJL*, 712, L69

Schneider, R., Ferrara, A., Salvaterra, R., Omukai, K., & Bromm, V. 2003, *Nature*, 422, 869

Schneider, R., Omukai, K., Limongi, M., et al. 2012, *MNRAS*, 423, L60

Schneider, R., Salvaterra, R., Ferrara, A., & Ciardi, B. 2006, *MNRAS*, 369, 825

Sethi, S., Haiman, Z., & Pandey, K. 2010, *ApJ*, 721, 615

Shang, C., Bryan, G. L., & Haiman, Z. 2010a, *MNRAS*, 402, 1249

Shang, C., Bryan, G. L., & Haiman, Z. 2010b, *MNRAS*, 402, 1249

Sugimura, K., Omukai, K., & Inoue, A. K. 2014, *MNRAS*, 445, 544

Susa, H., Hasegawa, K., & Tominaga, N. 2014, *ApJ*, 792, 32

Tanaka, K. E. I. & Omukai, K. 2014, *MNRAS*, 439, 1884

Toomre, A. 1964, *ApJ*, 139, 1217

Van Borm, C. & Spaans, M. 2013, *A&A*, 553, L9

Volonteri, M. & Bellovary, J. 2012, *Reports on Progress in Physics*, 75, 124901

Wutschik, S., Schleicher, D. R. G., & Palmer, T. S. 2013, *A&A*, 560, A34

Yoshida, N., Omukai, K., & Hernquist, L. 2008, *Science*, 321, 669

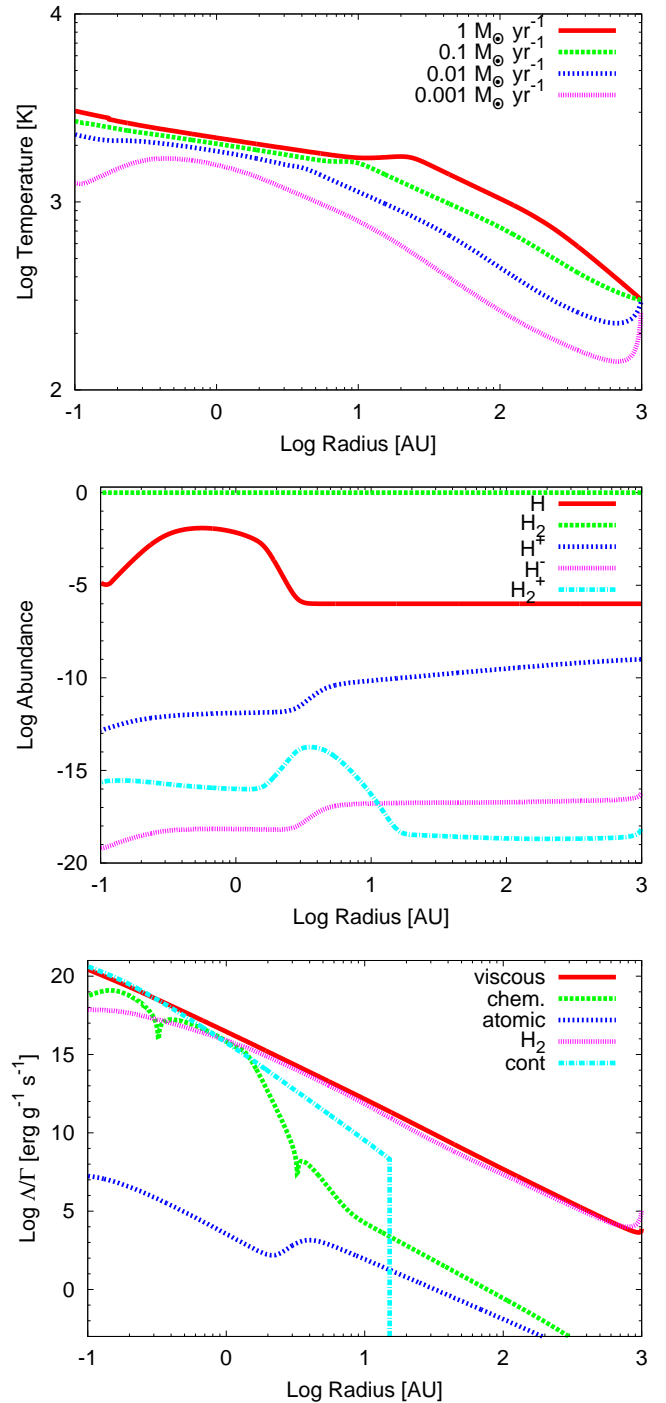


Fig. 1. Results for the generic disk models without central source and an initially molecular gas (Table 1). Top panel: Gas temperature vs radius in case of a generic disk model without central source, assuming different accretion rates. Mid panel: Abundances of H, H_2 , H^+ , H_2^+ , H^- vs radius for the reference case NS3 (disk with no source, accretion rate $10^{-3} M_{\odot} \text{ yr}^{-1}$). Bottom panel: Heating and cooling contributions vs radius for the reference case NS3 (disk with no source, accretion rate $10^{-3} M_{\odot} \text{ yr}^{-1}$). We refer to Table 3 for the heating/cooling contributions defined in the legend.

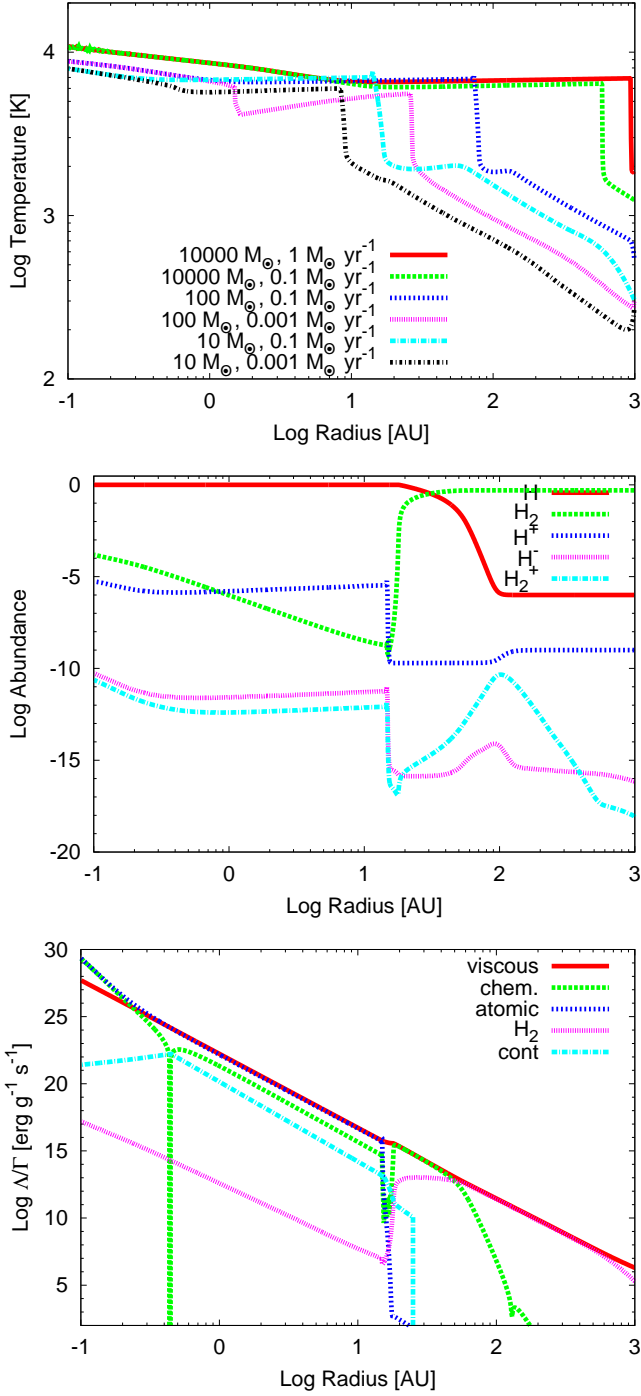


Fig. 2. Results for the generic disk models with central source and an initially molecular gas (Table 2). The species abundances and heating/cooling rates are given for the S2A3 (generic disk model with central source of $100 M_{\odot}$ and accretion rate of $10^{-3} M_{\odot} \text{ yr}^{-1}$). We refer to the caption of Fig. 1 for the description of the panels.

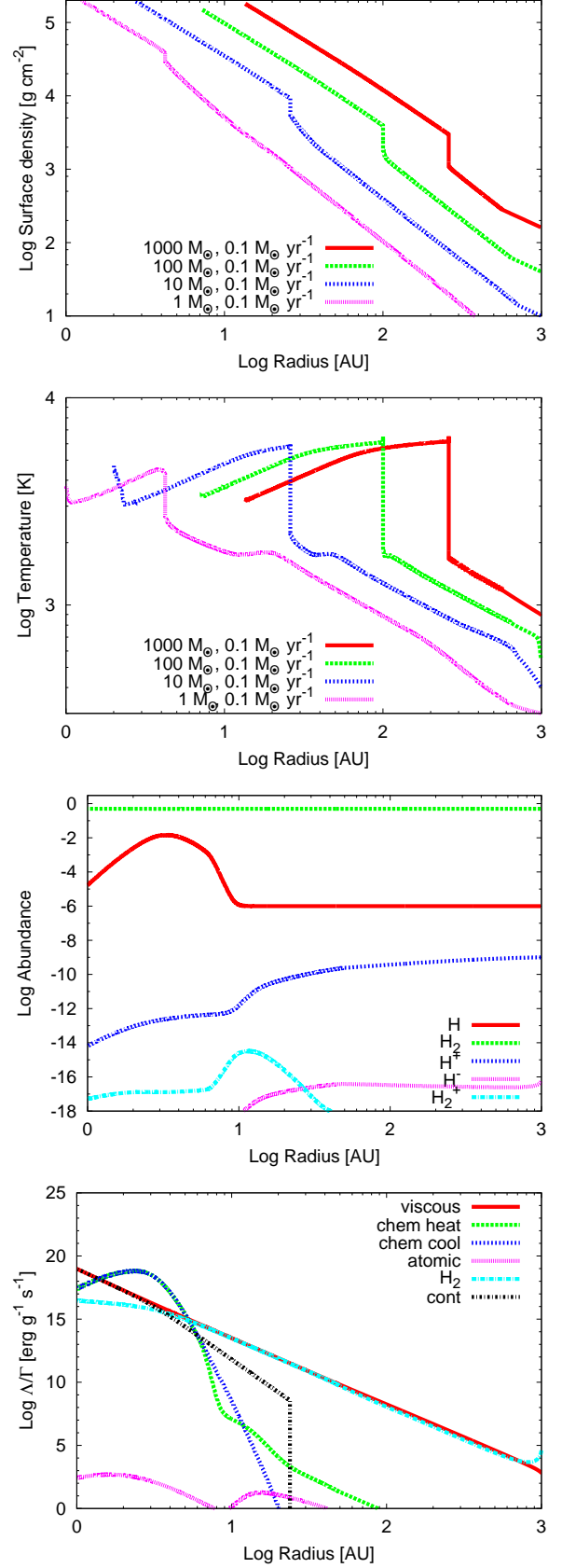


Fig. 3. Results for the self-regulated disk models with an initially molecular gas (Table 4), plus species abundances and heating/cooling rates for the reference case S1 (self-regulated disk with central source of $1 M_{\odot}$ and an accretion rate of $10^{-1} M_{\odot} \text{ yr}^{-1}$). The top panel shows the gas surface density as a function of radius. We refer to the caption of Fig. 2 for the description of the other panels.

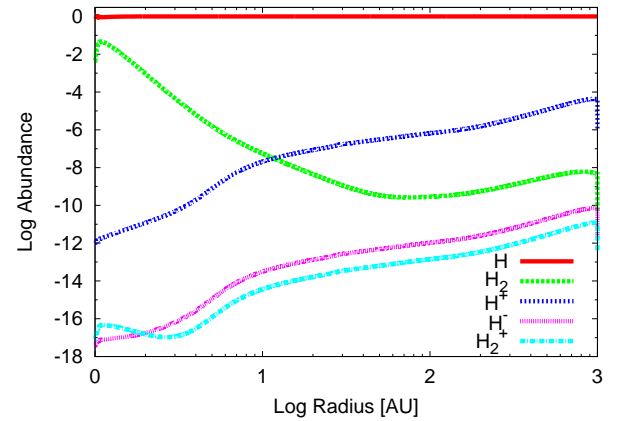
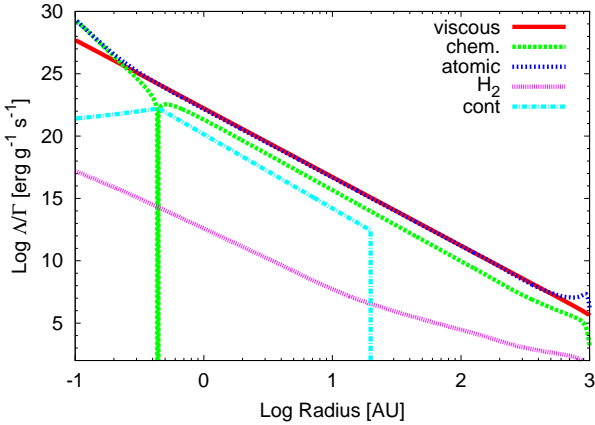
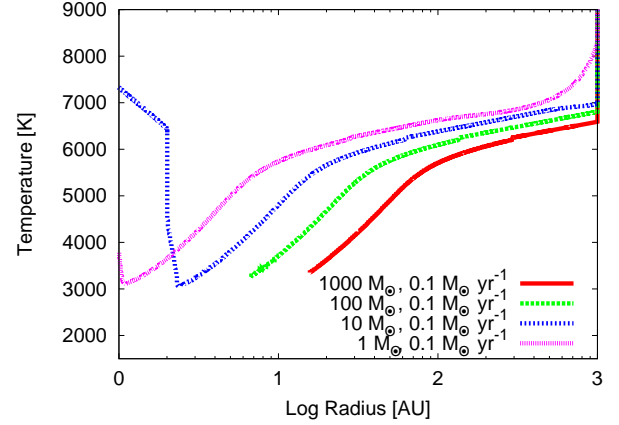
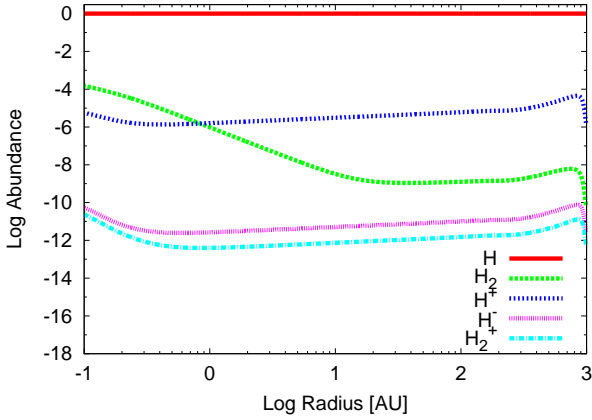
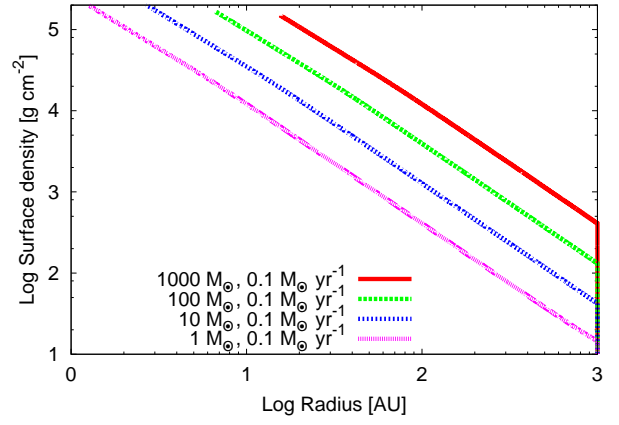
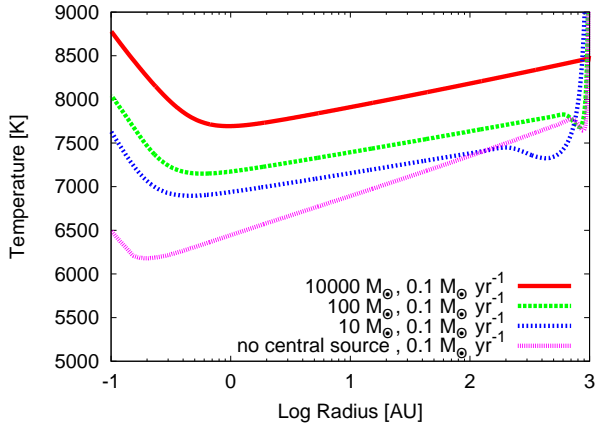


Fig. 4. Results for the generic disk model with an initially atomic gas (Table 5). The species abundances and heating/cooling rates are given for the H1 (generic disk model with central source of $10 M_{\odot}$ and an accretion rate of $10^{-1} M_{\odot} \text{ yr}^{-1}$). We refer to the caption of Fig. 1 for the description of the panels.

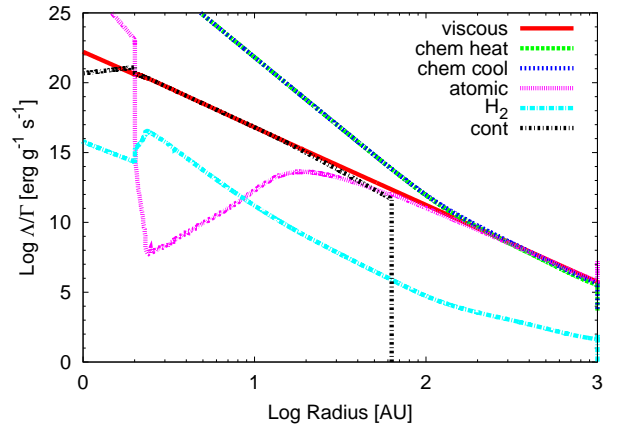


Fig. 5. Results for the self-regulated disk models with an initially atomic gas (Table 6). The species abundances and heating/cooling rates are given for the HS0 (self-regulated disk with central source of $1 M_{\odot}$ and an accretion rate of $10^{-1} M_{\odot} \text{ yr}^{-1}$). We refer to the caption of Fig. 3 for the description of the panels.